NUCLEAR SCIENCE AND ENGINEERING: **161**, 321–330 (2009)

Beryllium and Graphite High-Accuracy Total Cross-Section Measurements in the Energy Range from 24 to 900 keV

Y. Danon,* R. C. Block, M. J. Rapp, and F. J. Saglime

Rensselaer Polytechnic Institute
Department of Mechanical, Aerospace, and Nuclear Engineering
Troy, New York 12180-3590

and

G. Leinweber, D. P. Barry, N. J. Drindak, and J. G. Hoole

KAPL, Inc., Lockheed Martin Corporation
P.O. Box 1072, Schenectady, New York 12301-1072

Received February 25, 2008
Accepted July 4, 2008

Abstract—*This paper presents new measurements of the carbon and beryllium neutron total cross section in the energy range of 24 to 950 keV. The measurements were done using a pulsed neutron source driven by an electron LINAC. The neutron beam passed through a 30-cm-thick iron filter, which results in neutron transmission only in energies where resonance scattering and potential interference exist. The neutron filter removes most of the neutrons at other energies and significantly attenuates the gamma background resulting in 20 energy windows and a high signal-to-background ratio. The filtered beam was used for transmission measurements through graphite that results in ~1% accurate total cross sections that are in excellent agreement with current evaluations. The carbon measurement provides a verification of the accuracy of the filtered beam method. Measurements of three samples of different thicknesses of beryllium resulted in accurate total cross-section values that agree with one previous measurement and show discrepancies from current evaluations. The high accuracy of the new measurements can be used for improvement of future total cross-section evaluations of beryllium.*

I. INTRODUCTION

Beryllium is a lightweight metal that has physical and nuclear properties that make it desirable in several nuclear applications. Beryllium has a low thermal absorption cross section and has been used as a neutron reflector in compact high flux reactors such as the Advanced Test Reactor[1] (ATR). Because of its low atomic mass, beryllium can also be used as a moderator, and its light weight makes it favorable in space applications.[1] Beryllium also has applications in fusion both as a first-wall material and as blanket material utilizing the low threshold for the $(n, 2n)$ reaction.[2,3] Thus, accurate knowledge of the beryllium total neutron cross section is important for accurate design calculations for these applications.

A review of the evaluated total cross section of beryllium in the energy range from 10 to 1000 keV reveals ~8% discrepancy between the recent evaluations (see Fig. 1). A review of the existing data retrieved from EXFOR (Ref. 4) also shows discrepancies between the different measurements (see Fig. 2), which are also reflected in the evaluation. In order to resolve the discrepancies, an accurate measurement of the total cross section is required. The iron filtered beam method can provide such data and was used before at Rensselaer Polytechnic Institute[5,6] (RPI) for measurements of the total cross section of deuterium and measurement of the beryllium total

*E-mail: danony@rpi.edu

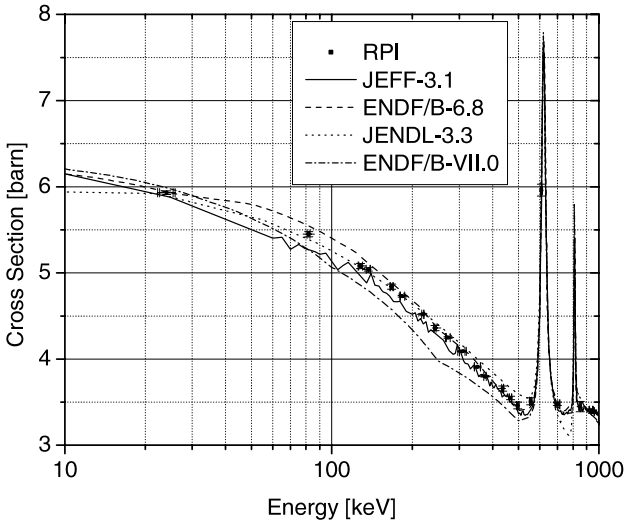

Fig. 1. The measured total cross section plotted with the ^{9}Be cross section from several evaluations.

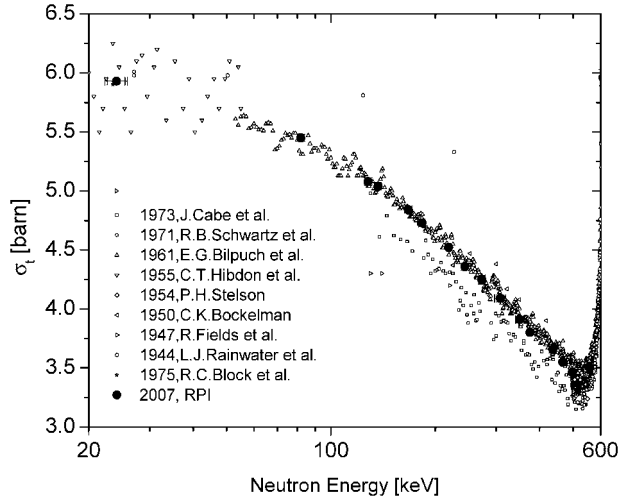

Fig. 2. The measured ^{9}Be data plotted with previously measured data. The new data are in good agreement with the Bilpuch et al.[26] data from 1961.

cross section[7] at 24 keV. More recently, the iron filtered beam method was used to study neutron scattering from water and heavy water.[8] A related method, the uranium filtered beam, was also recently used for scattering measurements from hydrogen[9] in CH_2, and a more in-depth review of this method is given elsewhere.[10]

In general, total cross-section measurements can be done using a pulsed neutron beam in a transmission geometry. The transmission through the sample is measured using the time-of-flight (TOF) technique, which allows the measurement of the energy-dependent total cross section $\sigma_t(E_i)$ by applying Eq. (1) for every TOF channel i:

$$\sigma_t(E_i) = \frac{-1}{N} \ln(T_i) \ , \tag{1}$$

where

T_i = transmission at TOF channel i

N = number density (atom/b).

The transmission is calculated from the sample-in and the sample-out count rates Rs_i and Ro_i, respectively, and their associated time-dependent background rates Bs_i and Bo_i:

$$T_i = \frac{Rs_i - Bs_i}{Ro_i - Bo_i} \ . \tag{2}$$

The most problematic aspect of the TOF technique is accurate determination of the time-dependent background count rate (Bs_i and Bo_i). The sources of background could be both neutrons and gamma rays. The neutron time-dependent background is mostly due to neutrons that interacted with the neutron producing target and moderator, and the collimation system, thus arriving at the detector at a TOF that is not correlated to the energy of the uncollided neutron beam. Similarly, the gamma background is a result of neutron interactions in the neutron producing target and moderator (for example, 2.2-MeV capture gammas from hydrogen in the moderator) and gammas from inelastic neutron scattering and capture interactions in the collimation system. Usually, a separate measurement (see Ref. 11, for example) is required in order to characterize the time-dependent background. These measurements can be done using strong resonance absorbers of two thicknesses and extrapolating the background to zero thickness. The accuracy of the background correction is a function of the signal-to-background ratio of a given TOF facility and the accuracy of the background measurement and analysis methods.

The filtered beam method has a great advantage in providing a high signal-to-background ratio. In this method a thick filter (30 cm of iron in the experiment reported here) is placed in the neutron beam. Most of the neutrons and gammas in the beam are completely attenuated by this thick filter. A filter material is selected such that the interference between the resonance and potential scattering results in total cross section minima in a desired energy range. Thus, the thick filter has "holes" through which neutrons of specific energies can stream. The transmission through the holes varies but, for 30 cm of iron, can reach 60% in some points. The resulting TOF spectrum exhibits peaks that can be used for transmission measurements at these specific energy windows.

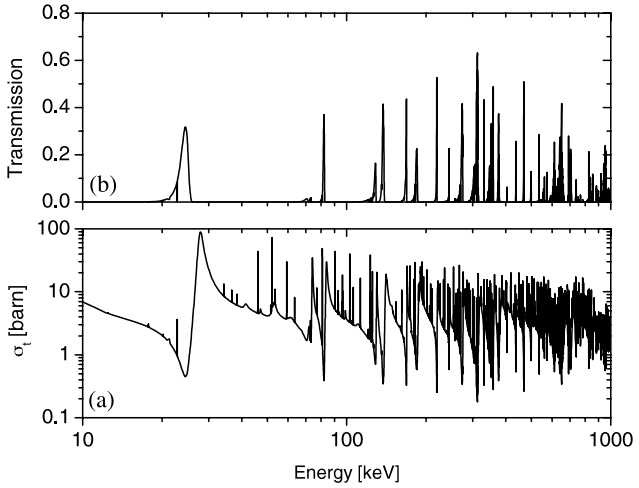

Fig. 3. (a) The total cross section [from ENDF/B-VI.8 (Ref. 14)] of natural Fe. (b) Calculated neutron transmission through 30 cm of iron, showing peaks (holes) through which neutrons at discrete energies pass through the iron filter.

The advantage of the filter is that it blocks the background neutrons and gammas and thus eliminates the need for a separate background measurement.

An iron filter with a thickness of 30 cm was used for the measurement of the Be cross section in the energy range from 24 to 950 keV. An example of the calculated transmission through 30 cm of Fe is show in Fig. 3.

A measurement of the total cross section of carbon (graphite) that is well known was used to benchmark the method followed by a measurement for several sample thicknesses of beryllium. Additional information on this experiment and preliminary data are given in Ref. 12.

II. EXPERIMENTAL SETUP

The experiments were performed at the Gaerttner Laboratory at RPI. The setup is illustrated in Fig. 4. Neutrons are produced by electrons hitting the RPI bare bounce target[13] placed on the neutron beam axis without an additional polyethylene moderator discussed in Ref. 13. The collimated neutron beam passes through a 30-cm iron filter and another stage of collimation where the beam diameter is reduced to 4.7625 cm (1.875 in.). The beam then passes through the sample being measured and continues to the neutron detector. The neutron flight path distance was 25.565 ± 0.005 m as was determined by a fit of the iron peaks to a calculation using the ENDF/B-VI.8 total cross section data[14] for ^{56}Fe. The source to sample distance was ~13.85 m, and the sample detector distance was ~11.71 m.

The RPI LINAC pulsed electron beam had an energy of 55 MeV, a 6-ns pulse width, and an average current of 4 ± 1 μA. The data collection time was 90 and 60 h for beryllium and graphite, respectively. The beam intensity was monitored by two fission chambers of which one was selected to normalize the data to eliminate the effect of beam intensity variations. A variety of statistical methods was used for selection of the best correlating monitor using the RPI MONCHK code.[15]

The detector was a 1.27-cm (0.5-in.)-thick and 12.7-cm (5-in.)-diam GS-20 Li-glass detector with a single out-of-the-beam Photonis XP4572B photomultiplier. The detector electronics were optimized using a fast (45-ns time constant) custom CREMAT preamp that fed an ORTEC 375 constant fraction discriminator. The time jitter of the system was ~1 ns measured by observing the time jitter between the gamma flash and the LINAC start pulse. The discriminator signal was used as a stop signal for a 7887 FastComTec TOF clock operating with 1.25 ns/channel and a total of 486 016 channels. The 7887 is a multihit TOF clock with no dead time between channels. The ORTEC discriminator blocking output was used as the TOF clock stop signal and was adjusted to a pulse width of 70 ns. The system dead time was determined in a separate experiment with the signal of the detector connected to both the start and stop of the TOF clock. In this configuration, the TOF spectrum from an ~3-Ci PuBe neutron source was collected. The TOF data

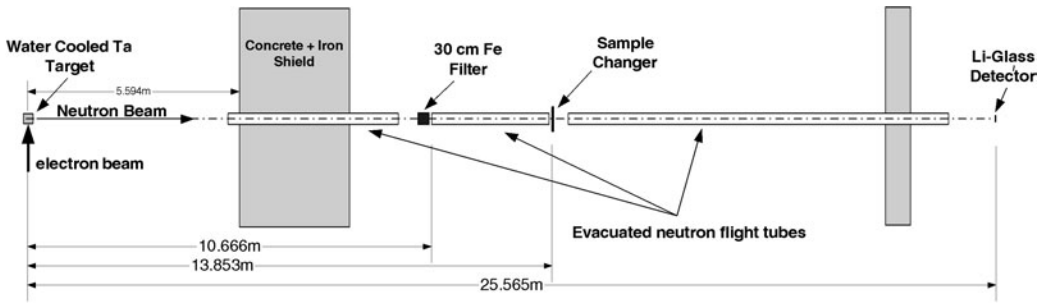

Fig. 4. The experimental setup showing the neutron producing target, iron filter, sample position, flight paths, and detector position.

allow determination of the system dead time, which was found to be 230 ± 30 ns. To ensure the dead-time correction error was minimal, the LINAC electron beam current was chosen such that at the maximum count rate, the dead-time correction factor was kept below 2% throughout the duration of the data collection.

Additional neutron detectors (Reuter-Stokes RS-P6-2403-121 and Amperex B300D fission chambers), located on the far east flight tube at a flight-path distance of ~8 m, were used to monitor the neutron beam intensity variations.

The data collection times dedicated for each sample thickness and for the open beam were selected using the optimization described in Ref. 16. Each sample was rotated in and out of the beam such that ~7 min was dedicated to the open beam measurement and ~15 min to measurement of the thickest sample in each 45-min cycle.

III. SAMPLES

There are four cylindrical samples, one graphite and three beryllium, each with a diameter of 7.493 cm (2.95 in.). The sample diameter and weight were measured several times in order to obtain an accurate value for the number density N and its associated error σ_N. The sample details are listed in Table I.

All the beryllium samples contained 99.9% beryllium. The thickness uniformity of the samples was <0.05%. A spectrographic analysis of the Be material used to make the samples is given in Table II.

The carbon material used was reactor-grade graphite. The samples were cut from a larger piece and were baked in an oven at 200°C for 24 h to drive humidity out of the sample. Weighing the sample before and after the heating treatment indicates that for the worst case of the 7-cm sample, 0.024% of the weight was removed by this process. A chemical analysis of the graphite sample is given in Table III. Possible boron content is a problem only at low neutron energies, and a measurement of its concentration was not done. The graphite thickness uniformity was 1.2%.

TABLE I

Sample Thickness and Number Density

Sample	Nominal Thickness (cm)	N (atom/b)	σ_N (atom/b)
Graphite	7	0.5924	0.0002
Beryllium	2	0.24684	0.00009
Beryllium	3	0.3670	0.0001
Beryllium	5	0.6168	0.0002

TABLE II

Impurities in the Beryllium Samples

Impurity	Weight Fraction (ppm)
Ag	<3
Al	<300
Ca	<20
Co	<3
Cr	<20
Cu	<70
Fe	<700
Mg	<5
Mn	<20
Mo	<20
Ni	<100
Pb	<20
Sc	<5
Si	<200
Ti	<80
U	<30
W	<50
Zn	<10
Zr	<10

TABLE III

Impurities in the Graphite Samples

Impurity	Weight Fraction (ppm)
Ash[a]	1180
Al	14
Ca	166
V	55
Ti	3
Cr	2
Fe	30
Ni	14

[a]Ash represents the incombustible content.

IV. DATA ANALYSIS AND RESULTS

The data were first checked for consistency using the MONCHK computer code.[15] This code performs a statistical analysis of the data to detect anomalous data and flags it for further examination. This computer code also computes the correlation between the beam monitors and the in-beam detector to allow selection of the best correlating monitor for data normalization. The error associated with the normalization is ~10% of the statistical error and thus contributed very little to the overall error. For each experiment (Be or graphite

samples), sample data and open beam data were collected in about 150 files that were dead-time corrected and summed using the RPI RPIXDR code.[17]

The beryllium experiments included a 7-cm-thick graphite sample that was used as a verification of the system performance. A typical plot of the open beam TOF spectrum is shown in Fig. 5.

Analysis of the data required integration of the counts over the peaks and correction for the background under the peak. The integration limits were nominally set to the full-width at one-tenth of the maximum (FWTM). The limits were then systematically adjusted by a computer program that varied the integration limits in order to minimize the statistical error in transmission. Results with integration limits that are wider than the FWTM were rejected and limited to the FWTM for smaller peaks with lower signal-to-background ratios. This procedure results in smaller integration widths. The procedure was repeated for all samples, and the widest set was selected and used on all samples including the open beam data. This procedure affected the integration limits of four peaks at energies 555.3, 609.3, 851.8, and 947.5 keV.

The background was calculated by integration of the wings of each of the peaks averaging the counts on each side and assuming a straight line between the points on either side of the peak. The background channels on the wings were kept identical for all samples and the open beam. An illustration of the process is shown in Fig. 6. The signal-to-background ratio was calculated as $(S - B)/B$, where S is the sum of counts under the peak and B is the area under the background curve both calculated between the limits E_1 and E_2 (as shown in Fig. 6). The signal-to-background ratio is plotted in Fig. 7, and in general the ratio decreases with energy. This is attributed to the higher cross section in the filter's total cross-section minima (resulting in lower transmission) and the degradation of the system's energy resolution. The resolution broadening adds a low-energy tail to the transmission peaks that extends under the adjacent lower-energy peak and results in what appears to be a higher background under the lower-energy peak. Thus, improvement of the energy resolution is expected to further reduce the background.

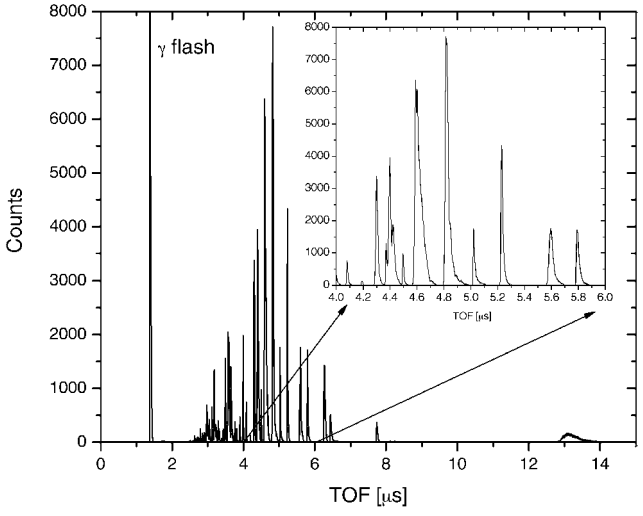

Fig. 5. TOF spectrum of the open beam data showing the peaks resulting from transmission through the iron filter. The TOF clock recorded the counts in channels of 1.25 ns/channel.

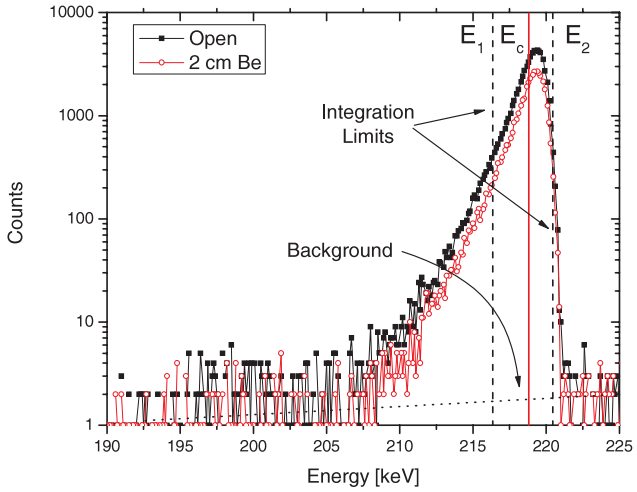

Fig. 6. Illustration of the background and integration limits (E_1 and E_2) shown on the 218.8-keV peak. The average energy E_c is calculated by Eq. (9). The background is determined by averaging several points on each side of the peak (not shown). The background under the peak is a straight line connecting two averaged background points on each side of the peak.

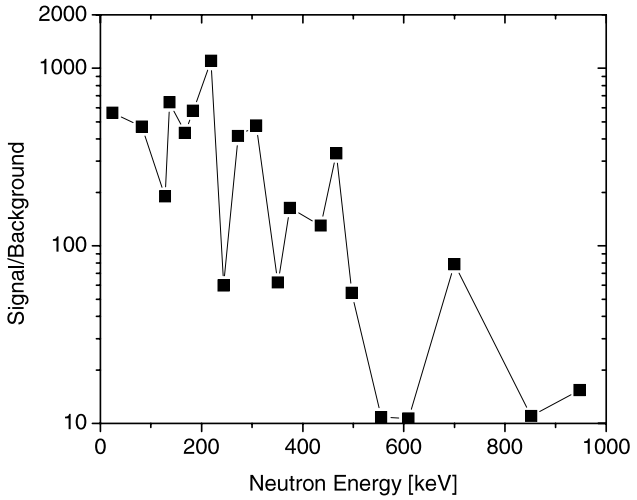

Fig. 7. The signal-to-background ratio as a function of neutron energy.

The effect of the integration limits on the accuracy of the cross section was estimated by calculating the limits at full-width of twice the original height (for example, FWTM changed to full-width at one-fifth of the maximum height). This resulted in a change in the cross section that is on the average different by 40% of the reported error and thus within the quoted errors.

The transmission for each of the samples was calculated by Eq. (3):

$$T = \frac{I_s}{I_o}\frac{M_o}{M_s} \quad , \tag{3}$$

where

I_s, I_o = background corrected integrated counts under the sample and open beam peaks, respectively

M_o, M_s = monitor counts for the open beam and sample, respectively.

The statistical error of the transmission ΔT was determined by simple error propagation assuming noncorrelated errors and is given by

$$\frac{\Delta T}{T} = \sqrt{\left(\frac{\Delta I_o}{I_o}\right)^2 + \left(\frac{\Delta I_s}{I_s}\right)^2 + \frac{1}{M_o} + \frac{1}{M_s}} \quad , \tag{4}$$

where ΔI_s and ΔI_o are the statistical errors in the background corrected counts for the sample and open beam, respectively.

The transmission data were converted to cross section using Eq. (1), and the error in the cross section $\Delta\sigma$ for each energy point of each sample thickness is calculated using Eq. (5):

$$\Delta\sigma = \frac{1}{N}\frac{\Delta T}{T} \quad . \tag{5}$$

The error in the number density N is small relative to the statistical error and was ignored.

A recommended cross-section value σ was obtained by a weighted average of n different sample thicknesses as given in Eq. (6):

$$\bar{\sigma} = \frac{\sum_{i=1}^{n} \frac{\sigma_i}{(\Delta\sigma_i)^2}}{\sum_{i=1}^{n} \frac{1}{(\Delta\sigma_i)^2}} \quad . \tag{6}$$

Two sources of error were considered in calculating the error in the recommended value. The first is the so-called internal error, which is the statistical error of the average given by

$$\Delta\sigma_{internal} = \left(\sum_{i=1}^{n} \frac{1}{(\Delta\sigma_i)^2}\right)^{-1/2} \quad . \tag{7}$$

The second error is the so-called external error resulting from differences between the samples of different thicknesses and is given by

$$\Delta\sigma_{external} = \sqrt{\frac{\sum_{i=1}^{n} \frac{(\bar{\sigma} - \sigma_i)^2}{(\Delta\sigma_i)^2}}{(\mathrm{n}-1)\sum_{\mathrm{i}=1}^{\mathrm{n}} \frac{1}{(\Delta\sigma_i)^2}}} \quad . \tag{8}$$

Note that the difference in the notation of Eq. (8) with the one in Ref. 18 is due to a typographical error[19] in Ref. 18. Reference 20 provides criteria to determine if the data from different samples can be considered statistically consistent and uses the Student's t-distribution to scale the errors. Reference 18 uses a different approach, which is to set the reported error to the maximum of the two errors $[\sigma = \max(\sigma_{internal}, \sigma_{external})]$, and because of its simplicity, this procedure was adopted in this analysis.

The average energy of each peak is calculated by Eq. (9) using the peak integration boundaries (see Tables IV and V) applied to the open beam data of beryllium:

$$E_c = \frac{\sum_{i=n_1}^{n_2} E_i C_i}{\sum_{i=n_1}^{n_2} C_i} \quad , \tag{9}$$

TABLE IV

Measured Graphite Transmission and Inferred Total Cross Section*

E_c (keV)	E_1 (keV)	E_2 (keV)	T	ΔT	σ_t (*b*)	$\Delta\sigma_t$ (b)
24.044	22.267	25.406	0.0630	0.0008	4.67	0.02
81.823	80.756	82.717	0.0729	0.0018	4.42	0.04
127.896	125.275	129.583	0.0758	0.0016	4.36	0.04
136.954	134.385	138.825	0.0773	0.0009	4.32	0.02
167.462	165.076	169.050	0.0814	0.0012	4.24	0.02
183.243	179.480	185.818	0.0848	0.0010	4.17	0.02
218.809	216.337	220.621	0.0905	0.0009	4.06	0.02
243.589	240.687	245.554	0.0921	0.0016	4.03	0.03
272.253	266.762	275.943	0.0967	0.0005	3.94	0.01
307.902	296.440	315.197	0.1033	0.0005	3.83	0.01
350.760	341.393	359.933	0.1081	0.0009	3.76	0.01
375.003	370.079	379.076	0.1131	0.0012	3.68	0.02
435.937	431.300	439.464	0.1178	0.0033	3.61	0.05
466.690	461.555	471.035	0.1281	0.0020	3.47	0.03
497.000	492.292	501.776	0.1330	0.0046	3.41	0.06
555.251	550.246	561.462	0.1447	0.0055	3.26	0.06
609.298	604.818	614.481	0.1492	0.0033	3.21	0.04
700.074	685.251	711.306	0.1703	0.0023	2.99	0.02
851.792	844.393	859.289	0.1850	0.0060	2.85	0.05
947.474	933.892	961.354	0.2095	0.0036	2.64	0.03

*The errors shown on the transmission and the total cross section are absolute 1σ values.

TABLE V

Measured Beryllium Transmission and Inferred Total Cross Section*

Energy			2 cm				3 cm				5 cm				Average	
E_c (keV)	E_1 (keV)	E_2 (keV)	T	ΔT	σ_t (b)	$\Delta\sigma_t$ (b)	T	ΔT	σ_t (b)	$\Delta\sigma_t$ (b)	T	ΔT	σ_t (b)	$\Delta\sigma_t$ (b)	σ_t (b)	$\Delta\sigma_t$ (b)
24.044	22.267	25.406	0.232	0.002	5.92	0.03	0.1113	0.0011	5.93	0.03	0.0258	0.0005	5.93	0.03	5.93	0.02
81.823	80.756	82.717	0.261	0.004	5.44	0.06	0.1336	0.0025	5.44	0.05	0.0345	0.0012	5.46	0.06	5.45	0.03
127.896	125.275	129.583	0.284	0.004	5.10	0.06	0.1531	0.0024	5.07	0.04	0.0439	0.0012	5.07	0.04	5.08	0.03
136.954	134.385	138.825	0.289	0.002	5.03	0.03	0.1548	0.0014	5.04	0.03	0.0448	0.0007	5.04	0.03	5.04	0.02
167.462	165.076	169.050	0.307	0.003	4.79	0.04	0.1680	0.0018	4.82	0.03	0.0493	0.0009	4.88	0.03	4.84	0.03
183.243	179.480	185.818	0.313	0.002	4.71	0.03	0.1746	0.0015	4.72	0.02	0.0536	0.0008	4.74	0.02	4.73	0.01
218.809	216.337	220.621	0.326	0.002	4.54	0.03	0.1889	0.0014	4.51	0.02	0.0611	0.0007	4.53	0.02	4.52	0.01
243.589	240.687	245.554	0.342	0.004	4.35	0.05	0.2024	0.0026	4.32	0.04	0.0661	0.0013	4.41	0.03	4.36	0.03
272.253	266.762	275.943	0.352	0.001	4.23	0.02	0.2079	0.0009	4.25	0.01	0.0720	0.0005	4.27	0.01	4.25	0.01
307.902	296.440	315.197	0.364	0.001	4.10	0.01	0.2203	0.0008	4.09	0.01	0.0807	0.0004	4.08	0.01	4.09	0.01
350.760	341.393	359.933	0.381	0.002	3.91	0.02	0.2348	0.0013	3.92	0.02	0.0899	0.0008	3.91	0.01	3.91	0.01
375.003	370.079	379.076	0.394	0.003	3.77	0.03	0.2445	0.0019	3.81	0.02	0.0957	0.0011	3.80	0.02	3.80	0.01
435.937	431.300	439.464	0.408	0.008	3.64	0.08	0.2542	0.0051	3.70	0.05	0.1062	0.0030	3.64	0.05	3.66	0.03
466.690	461.555	471.035	0.417	0.004	3.55	0.04	0.2662	0.0031	3.58	0.03	0.1140	0.0019	3.52	0.03	3.55	0.02
497.000	492.292	501.776	0.421	0.010	3.51	0.10	0.2806	0.0071	3.44	0.07	0.1190	0.0043	3.45	0.06	3.46	0.04
555.251	550.246	561.462	0.413	0.011	3.58	0.11	0.2740	0.0076	3.50	0.08	0.1166	0.0046	3.48	0.06	3.51	0.04
609.298	604.818	614.481	0.238	0.004	5.82	0.07	0.1082	0.0024	6.01	0.06	0.0242	0.0010	6.04	0.07	5.96	0.07
700.074	685.251	711.306	0.423	0.004	3.48	0.04	0.2751	0.0030	3.49	0.03	0.1174	0.0018	3.47	0.03	3.48	0.02
851.792	844.393	859.289	0.424	0.014	3.48	0.13	0.2804	0.0097	3.44	0.09	0.1189	0.0060	3.45	0.08	3.45	0.06
947.474	933.892	961.354	0.430	0.006	3.42	0.06	0.2841	0.0041	3.40	0.04	0.1256	0.0024	3.36	0.03	3.39	0.02

*The errors shown on the transmission and the total cross section are absolute 1σ values.

where

n_1, n_2 = channels corresponding to the integration boundary energies

E_i = channel energy

C_i = number of counts in channel i.

This average energy does not coincide with the peak energy because the shape of the peak is not symmetric, as illustrated in Fig. 6.

IV.A. Carbon

A 7-cm-thick graphite sample was measured in order to study the accuracy of the iron filtered beam method. The data were compared to the ENDF/B-VII.0 evaluation,[21] which is based on numerous previous measurements. The data for carbon are shown in Table IV. The cross section is plotted in Fig. 8a together with the ENDF/B-VII.0 cross section for ^{12}C, which was linearly interpolated between the ENDF/B-VII.0 points. Figure 6b shows the fractional difference between our experiment and ENDF/B-VII.0 for all measured data points with the experimental error of 1% or lower; 14 of 20 points are within 1% of the evaluation. The remaining six data points all have statistical errors <2% and are within 2% of the evaluation. This observation verifies that the procedures used for the measurement and data reduction provide a good central value and a good estimate of the experimental error even for a small 1% error. The largest cross-section error in the graphite measured data is 1.8%. Table IV also provides the low- and high-energy boundaries for each of the peaks. Because the cross section is a weighted average of the peak profile (see Fig. 6) and the sample cross section, these boundaries provide an energy error estimate for each data point.

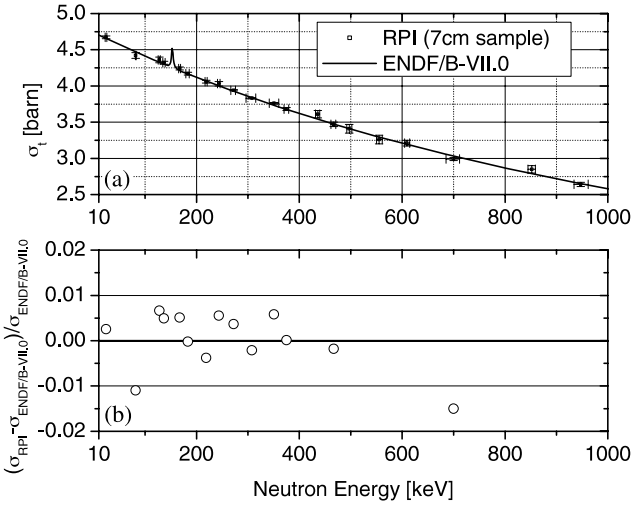

Fig. 8. (a) Measured carbon cross section compared with the ENDF/B-VII.0 evaluation. (b) Experimental data with statistical error of <1% are compared with the relative difference to the ENDF/B-VII.0 evaluation for ^{12}C.

IV.B. Beryllium

Data were collected for three sample thicknesses of Be (2, 3, and 5 cm). The data analysis was done using the same procedure as the graphite sample, as outlined in Sec. IV.A. The data are shown in Table V. The overall accuracy of most of the data points is ~1% (see last two columns of Table V). The data are plotted in Fig. 1 together with several ^{9}Be evaluations. The first observation is that all the evaluations have about the same value at 24 keV, which includes the data point (5.90 ± 0.01 b) based on the older KURRI iron filtered beam measurement.[7] This point is in good agreement with the new data (5.93 ± 0.02 b). Below 300 keV the new data are in agreement with JENDL 3.3 (Ref. 22) while above 300 keV the agreement with JEFF 3.1 (Ref. 23) is better. Below 550 keV, ENDF/B-VII.0 is much lower than the other evaluations.

Comparisons with measured data[7,24–31] are shown in Fig. 2. The RPI measurement is in very good agreement with the data of Bilpuch et al.[26] In the region of 200 to 500 keV, the current data are slightly lower than the Bilpuch et al. data. The other measurements exhibit large differences from these two sets.

V. CONCLUSIONS

This paper presents new total cross-section measurements of carbon and beryllium in the energy range from 24 to 950 keV using an iron filtered neutron beam generated by an electron LINAC. The filtered neutron beam is generated by passing the neutrons though 30 cm of iron. The scattering resonance potential interference results in minima in the iron total cross section, which creates holes through which neutrons of appropriate energy can be transmitted. Transmission measurements were done with carbon and beryllium samples that were placed in the filtered beam. The advantage of the filtered beam method is the high signal-to-background ratio that can be achieved because the iron filter removes most of the gamma background and neutrons at energies other than filter cross-section minima. The disadvantage is that only 20 points in the whole energy range can be obtained, and thus, this method is most appropriate for smooth cross sections.

Because the carbon cross section is well known, measurements with reactor-grade graphite were used to benchmark the method and yielded excellent agreement with ENDF/B-VII.0 with accuracy of ~1% for several of the measured points. Measurements of the Be cross sections are in general agreement with JENDEL 3.3, JEFF 3.1, and ENDF/B-VI.8, which agree with each other within a

few percent. The more recent ENDF/B-VII.0 evaluation is lower than the previous evaluations and the new data by up to 8%. This new high-accuracy measurement can help reduce the uncertainty in the ^{9}Be cross section in the measured energy range. It also provides a good verification for the ^{12}C evaluations.

REFERENCES

1. T. A. TOMBERLIN, "Beryllium—A Unique Material in Nuclear Applications," *Proc. 36th SAMPE Int. Technical Conf.*, San Diego, California, November 15–18, 2004, Society for the Advancement of Material and Process Engineering (2004).

2. H. KAWAMURA, H. TAKAHASHI, N. YOSHIDA, V. SHESTAKOV, Y. ITO, M. UCHIDA, H. YAMADA, M. NAKAMICHI, and E. ISHITSUKA, "Application of Beryllium Intermetallic Compounds to Neutron Multiplier of Fusion Blanket," *Fusion Eng. Des.*, **61–62**, 391 (Nov. 2002).

3. J. PAMÉLA, F. ROMANELLI, M. L. WATKINS, A. LIOURE, G. MATTHEWS, V. PHILIPPS, T. JONES, A. MURARI, A. GÉRAUD, F. CRISANTI, R. KAMENDJE, and JET-EFDA CONTRIBUTORS, "The JET Programme in Support of ITER," *Fusion Eng. Des.*, **82**, *5–14*, 590 (Oct. 2007).

4. "EXFOR Systems Manual: Nuclear Reaction Data Exchange Format," BNL-NCS-63330, V. McLANE, Ed., Nuclear Data Centers Network, National Nuclear Data Center, Brookhaven National Laboratory (1996).

5. P. STOLER, N. N. KAUSHAL, F. GREEN, E. HARMS, and L. LAROZE, "Total Neutron Cross Section of Deuterium Below 1000 keV," *Phys. Rev. Lett.*, **29**, 1745 (1972).

6. P. STOLER, N. N. KAUSHAL, and F. GREEN, "Total Cross Section of Neutrons on Deuterium in the keV Region," *Phys. Rev. C*, **8**, *4* (Oct. 1973).

7. R. C. BLOCK, Y. FUJITA, K. KOBAYASHI, and T. OOSAKI, "Precision Neutron Total Cross-Section Measurements Near 24 keV," *J. Nucl. Sci. Technol.*, **12**, 1 (1975).

8. R. MOREH, R. C. BLOCK, Y. DANON, and M. NEUMANN, "Search for Anomalous Scattering of keV Neutrons from H_2O-D_2O Mixtures," *Phys. Rev. Lett.*, **94**, 185301 (2005).

9. R. MOREH, R. C. BLOCK, Y. DANON, and M. NEUMAN, "Scattering of 64 eV to 3 keV Neutrons from CH_2 and Graphite and the Coherence Length Problem," *Phys. Rev. Lett.*, **96**, 055302 (2006).

10. R. MOREH, R. C. BLOCK, and Y. DANON, "Generating a Multi-Line Neutron Beam Using an Electron Linac and a U-Filter," *Nucl. Instrum. Methods Phys. Res. A*, **562**, *1*, 401 (2006).

11. D. B. SYME, "The Black and White-Filter Method for Background Determination in Neutron Time-of-Flight Spectrometry," *Nucl. Instrum. Methods*, **198**, 357 (1982).

12. Y. DANON, R. C. BLOCK, M. RAPP, F. SAGLIME, D. P. BARRY, N. J. DRINDAK, J. HOOLE, and G. LEINWEBER, "High-Accuracy Filtered Neutron Beam and High-Energy Transmission Measurements at the Gaerttner Laboratory," *Proc. Int. Conf. Nuclear Data for Science and Technology*, Nice, France, April 22–27, 2007.

13. M. E. OVERBERG, B. E. MORETTI, R. E. SLOVACEK, and R. C. BLOCK, "Photoneutron Target Development for the RPI Linear Accelerator," *Nucl. Instrum. Methods Phys. Res. A*, **438**, 253 (1999).

14. "ENDF-6 Formats Manual: Data Formats and Procedures for the Evaluated Nuclear Data File ENDF/B-VI and ENDF/B-VII," BNL-NCS-44945-05-Rev, Document ENDF-102, M. HERMAN, Ed., Brookhaven National Laboratory (June 2005).

15. Y. DANON, PhD Thesis, Rensselaer Polytechnic Institute (1993).

16. Y. DANON and R. C. BLOCK, "Minimizing the Statistical Error of Resonance Parameters and Cross Sections Derived from Transmission Measurements," *Nucl. Instrum. Methods A*, **485**, 585 (June 2002).

17. Y. DANON, "Rensselaer Polytechnic Institute Cross-Section Data Reduction Computer Code (RPIXDR 1.10.1)," Rensselaer Polytechnic Institute (2006).

18. S. F. MUGHABGHAB, *Atlas of Neutron Resonances*, Elsevier Science (2006).

19. S. F. MUGHABGHAB, Personal Communication (2007).

20. YU. F. YABOROV, "Method for Evaluating Non-Consistent Data Using Two Statistical Criteria," INDC(CCP)-343, International Nuclear Data Committee (1991).

21. M. B. CHADWICK et al., "ENDF/B-VII.0: Next Generation Evaluated Nuclear Data Library for Nuclear Science and Technology," *Nucl. Data Sheets*, **107**, 2931 (2006).

22. K. SHIBATA, T. KAWANO, T. NAKAGAWA, O. IWAMOTO, J. KATAKURA, T. FUKAHORI, S. CHIBA, A. HASEGAWA, T. MURATA, H. MATSUNOBU, T. OHSAWA, Y. NAKAJIMA, T. YOSHIDA, A. ZUKERAN, M. KAWAI, M. BABA, M. ISHIKAWA, T. ASAMI, T. WATANABE, Y. WATANABE, M. IGASHIRA, N. YAMAMURO, H. KITAZAWA, N. YAMANO, and H. TAKANO, "Japanese Evaluated Nuclear Data Library Version 3 Revision-3: JENDL-3.3," *J. Nucl. Sci. Technol.*, **39**, 1125 (2002).

23. A. KONING, R. FORREST, M. KELLETT, R. MILLS, H. HENRIKSSON, and Y. RUGAMA, "The JEFF-3.1 Nuclear Data Library," JEFF Report 21 (2006).

24. J. CABE and M. CANCE, "Measurements of the Neutron Total Cross-Sections of Be, B-11, C, Al, Si, S, Ti, V, Ni, U-235, U-238, Pu-239 Between 100 kev and 6 Mev," Centre d'Etudes Nucléaires, Saclay, report 4524 (1973); data retrieved from the CSISRS database, file EXFOR 20480024 (Aug. 9, 2007).

25. R. B. SCHWARTZ and R. A. SCHRACK, "Total Neutron Cross Sections of Silicon and Beryllium," *Bull. Am. Phys. Soc.*,

16, 495(AH3) (1971); data retrieved from the CSISRS database, file EXFOR 20480024 (Aug. 9, 2007).

26. E. G. BILPUCH, J. A. FARRELL, G. C. KYKER, and P. B. PARKS, "Average Total Neutron Cross Sections," Washington Atomic Energy Commission Office Report 1034, p. 10 (1961); data retrieved from the CSISRS database, file EXFOR 11011003 (Aug. 9, 2007).

27. C. T. HIBDON and A. LANGSDORF, "Total Neutron Cross Sections in the keV Region, Be, B, C, F, Ti, Ni and Bi," *Phys. Rev.*, **98**, 223(B3) (1955); data retrieved from the CSISRS database, file EXFOR 11244002 (Aug. 9, 2007).

28. P. H. STELSON, 1954, data retrieved from the CSISRS database, file EXFOR 11242002 (Aug. 9, 2007).

29. C. K. BOCKELMAN, "Total Cross Sections of Be, B, O and F for Fast Neutrons," *Phys. Rev.*, **80**, 1011 (1950); data retrieved from the CSISRS database, file EXFOR 11208002 (Aug. 9, 2007).

30. R. FIELDS, B. RUSSELL, D. SACHS, and A. WATTENBERG, "Total Cross Sections Measured with Photo-Neutrons," *Phys. Rev.*, **71**, 508 (1947); data retrieved from the CSISRS database, file EXFOR 11260002 (Aug. 9, 2007).

31. L. J. RAINWATER and W. W. HAVENS, Jr., "The Slow Neutron Transmission of Be Metal as Measured by a Neutron Beam Spectrometer in the Energy Region 0.004 eV to 50 eV," Report 2269, Chicago University Metallurgical Laboratory (1944); data retrieved from the CSISRS database, file EXFOR 11258002 (Aug. 9, 2007).